JOURNAL OF MATERIALS SCIENCE 28 (1993) 4994–5001

A macrokinetic approach to crystallization modelling of semicrystalline thermoplastic matrices for advanced composites

A. MAFFEZZOLI, J. M. KENNY, L. NICOLAIS
Department of Materials and Production Engineering, University of Naples, P. Tecchio, 80125 Naples, Italy

A theoretical macrokinetic model for the crystallization of polyphenylene sulphide (PPS) matrix for high performance composites is presented. The model, accounting for the induction time due to nucleation, is able to predict crystallization changes in isothermal and non-isothermal conditions, including cold and melt crystallization, and quenching effects. Moreover, a simple expression is proposed for the temperature dependence of the kinetic constant allowing a straightforward calculation of model parameters. Theoretical results are in good agreement with calorimetric experimental data obtained in a wide range of thermal conditions. Time temperature transformation plots, constructed from the model developed for isothermal (TTT) and non-isothermal (CCT) conditions, are presented providing a fundamental tool for understanding the crystallization behaviour of semicrystalline matrices and to determine the most appropriate processing conditions.

1. Introduction

Semicrystalline thermoplastic polymers have been proposed as an alternative to thermosets as matrices for high performance composites, showing many advantages in terms of properties and processing [1]. Fabrication of semicrystalline thermoplastic based composites is performed by heating the system over the melting temperature of the matrix under controlled conditions. Then the material is shaped by pressure application and, finally, the formed parts are cooled down to room temperature leading to the formation of the crystalline structure, responsible for the final physical properties of the composite. Usual processing conditions can involve cooling rates of the order of several hundred degrees centigrade per minute, leading to amorphous regions characterized by weaker mechanical properties and poor thermal and environmental resistances [2–6]. Therefore, temperature and crystallinity profiles during processing of semicrystalline matrix composites must be optimized. Comprehension of the crystallization behaviour of matrices for advanced composites like PEEK (polyether ether ketone), PPS (polyphenylene sulphide) or TPI (thermoplastic polyimide) is a fundamental starting point for process simulation and optimization.

Although the kinetics of polymer crystallization have been studied for a long time [7, 8], many experimental and theoretical questions are still unsolved as a consequence of the complexity of the nucleation and growth phenomena of macromolecular crystals. In particular, the melting history of a polymer can modify the crystallization kinetic acting on the nucleation process, altering the polymer structure due to branching, partial cross-linking or degradation phenomena [9, 10]. Moreover, as a consequence of experimental restrictions of the currently available techniques, the crystallization kinetics can normally be analysed only over a narrow temperature interval and under low cooling rates. In the case of composite materials, the effect of the fibres must also be considered. Fibres may act on crystallization as nucleating agents, modifying the crystal morphology and reducing the maximum degree of crystallinity as a consequence of the steric hindrance offered to crystal growth [4, 11–14].

The aim of this work is to develop a simple macrokinetic model for crystallization of composite matrices that can be used for process modeling. The main objective of the theoretical model is the description of the crystallization behaviour of thermoplastic matrices during processing under normal thermal conditions, including cold and melt crystallization, and quenching.

The results of the calorimetric characterization of a polyphenylene sulphide (PPS) matrix/carbon fibre composite, in a wide range of thermal conditions, are used for testing the model.

2. Crystallization models

The macrokinetics of the isothermal crystallization of semicrystalline polymers has been extensively reported in the scientific literature [7], adopting simple models that can be reduced in almost all cases to the Avrami equation

$$X_r(t) = 1 - \exp[-kt^n] \quad (1)$$

0022–2461

where X_r is the relative volume fraction of crystallinity with reference to the final amount of crystallinity developed over long periods of time, n is the Avrami exponent and k is the kinetic constant.

Non-isothermal crystallization has traditionally been approached by starting from the classical Avrami model and obtaining integral or differential expressions with a temperature dependent kinetic constant. Nakamura *et al.* [15] proposed the following integral expression obtained from the general Avrami theory

$$X_r(t) = 1 - \exp\left[- \int_0^t K(T)\, dt \right]^n \quad (2)$$

$K(T)$ is related to the Avrami constant through the relation $K(t) = k(T)^{1/n}$. Evidently, Equation 2 reduces to the Avrami equation under isothermal conditions.

A differential expression of the Nakamura model, more suitable for kinetic studies and for process modeling, was obtained by Patel and Spruiell [16]

$$dX_r/dt = nK(T)(1 - X_r) \times \{\ln[1/(1 - X_r)]\}(n - 1)/n \quad (3)$$

Another integral expression, developed by Kamal and Chu [17], was later applied to the non-isothermal crystallization of PEEK by Velisaris and Seferis [2]

$$X_r = 1 - \exp\left[- \int_0^t k(T) n t^{n-1} dt \right] \quad (4)$$

Lin [18] reported the differential expression of the Kamal model

$$dX_r/dt = nk(T)(1 - X_r)t^{(n-1)} \quad (5)$$

Although this expression was developed independently, it can be transformed into the Avrami equation if integrated at constant temperature.

Furthermore, the Ozawa [19] model must be mentioned as one of the first attempts to obtain a non-isothermal expression of crystallization

$$\ln[1 - X_r] = \chi(T)/R^n \quad (6)$$

where R is the cooling rate, χ is a temperature dependent parameter and n has the same meaning as the Avrami exponent. This equation, that can also be obtained from the Nakamura model (Equation 2), allows calculation of the Avrami exponent when a constant rate R is used.

While all the precedent models can be reduced to the classical Avrami expression under isothermal conditions, Malkin *et al.* [20, 21] proposed a completely different approach, describing crystallization as an autocatalytic process

$$dX/dt = K_m(X_{eq} - X)(1 + C_0X) \quad (7)$$

Where K_m and C_0 are temperature dependent parameters, X is the absolute crystallinity volume fraction and X_{eq} is the equilibrium degree of crystallinity developed.

For crystallization processes occurring through two different mechanisms, expressions obtained by combining in series or in parallel the above equations have been reported [2, 7, 17, 22, 23].

Patel and Spruiell [16] recently analysed the available methods describing non-isothermal crystallization in the framework of process modeling. They obtained a better fit for non-isothermal data by applying Equation 3, rather than its integral form (Equation 2), and attributed this result to the absence of time as an independent variable in Equation 2. Indeed, considering that Equation 3 can be deduced from Equation 2, the same results should be obtained by using either of these two equations if the correct onset time for crystallization is used. When this onset time is not correctly determined, different results are obtained from these two equations and Equation 3 better represents the experimental data using the initial conditions indicated by Patel and Spruiell [16]. However, as they recognized, the Nakamura model in both forms overpredicts the non-isothermal data, because it does not account for the induction time due to the nucleation process.

2.1. Temperature dependence

Considering that the crystallization kinetic constant is proportional to the crystal linear growth rate, G [7], its temperature dependence may be obtained from the theory developed by Hoffman *et al.* [8]. They proposed the following relationship between G and T

$$G = G_0 \exp[- U/R(T - T_\infty)] \times \exp[- K_g/T\Delta Tf] \quad (8)$$

where G_0 is a pre-exponential factor. The first exponential, named the retardation factor, accounts for the reduction of molecular mobility when the temperature approaches T_∞ and the second accounts for the driving force of crystallization, given primarily by the degree of undercooling $\Delta T = T_m^0 - T$ with respect to the theoretical melting point T_m^0. T_∞ represents a hypothetical temperature where all motion associated with viscous flow is hindered. Hoffman *et al.* [8] took a value of T_∞ lower than the glass transition temperature, T_g, according to the William-Landel-Ferry (WLF) theory for the temperature dependence of viscosity ($T_\infty = T_g - 51.2\,^\circ C$). K_g is a function of the surface free energy of the crystals and of the heat of crystallization, U is an activation energy for molecular motion, and the factor $f = 2T/(T + T_m^0)$ accounts for the reduction in the heat of crystallization as a function of temperature.

Following the proportionality between k and G, Equation 8 can be adapted to represent the macrokinetic behaviour of the kinetic constant

$$k = k_0 \exp[- E/R(T - T_\infty)] \times \exp[- C/T\Delta Tf] \quad (9)$$

This equation is widely used in the literature, often omitting the factor f [2, 7, 16, 21, 23, 24]. However, the presence in Equation 9 of several parameters that have lost their physical meaning when going from microkinetics (Equation 8) to macrokinetics (Equation 9), constitutes a limitation for its effective application. In this work a simplified version of Equation 9 to describe the processing of semicrystalline matrix composites is proposed.

In the microkinetic approach (Equation 8), the first exponential, as mentioned above, is obtained by adapting the WLF theory for the bulk viscosity. However the values of U and T_∞ that apply to bulk fluidity are not necessarily the same as those that apply to the crystallization process. In fact, the values of U and T_∞ applicable to crystallization are not related to the true viscosity of the amorphous phase, but probably refer to motions near and within a physically adsorbed layer of molecules that are confined to the surface of crystals. Therefore crystallization, at temperatures close to T_g, is governed by molecular motions associated with a viscosity higher than that of the amorphous phase at the same temperature. For these reasons crystallization in polymers cannot occur at the glass transition or lower temperatures, where molecular motions are hindered. Hence, in the macroscopic approach represented by Equation 9 it is more practical to use T_g rather than T_∞, reducing the number of parameters. Based on these considerations, a simpler expression for a macrokinetic approach will be proposed in this work for the temperature dependence of k.

2.2. Nucleation process

Nucleation is heterogeneous in nature in most polymers used for commercial applications, since nucleation agents are usually added in order to accelerate the overall crystallization process [7, 23, 25]. Moreover, in polymer composites fibre surfaces can act as nucleating agents, significantly contributing to heterogeneous nucleation [13, 14]. Heterogeneous nucleation is a thermally activated phenomenon and its effect is macroscopically detected by isothermal DSC experiments as an induction time before the crystal growth starts [7]. The induction time is not easily detected in non-isothermal crystallization experiments, but it plays a fundamental role determining the onset time for crystal growth. Crystallization models that neglect the effects of nucleation lead to unsatisfactory results. In fact, Velisaris and Seferis [2] introduced two fictive crystallization onset temperatures for each growth mechanism of the PEEK matrix, in order to overcome the absence of the induction time in their model. For the same material, Cebe [23], neglecting nucleation, included a dependence on the cooling rate of the Ozawa model parameters, enhancing the complexity of the model. For the same reasons, Patel and Spruiell [16], using the Nakamura model for crystallization of nylon 6, overestimated the non-isothermal experimental data.

According to Wunderlich [7] the nucleation rate I^* (number of nuclei per unit time and volume) can be expressed using an expression similar to Equation 8

$$I^* = I_0^* \exp[-\Delta G^*/k\Delta T f] \times \exp[-\Delta G_\eta/R(T - T_\infty)] \quad (10)$$

where ΔG^* represents the free enthalpy of crystallization of a nucleus of critical size and ΔG_η the free enthalpy of activation which governs the diffusion of the crystallizing element across the phase boundary. Again, as in the crystallization growth process, the pulling forces for nucleation are substantially given by the temperature differences $\Delta T = T_m^0 - T$ and $T - T_\infty$, showing opposite behaviour and originating a bell-shaped curve for I^*.

3. Experimental procedure

Thermal analysis experiments were performed on a PPS prepreg, Ryton AC-66, reinforced with 60% carbon fibres, kindly provided by Phillips Petroleum Co. The evolution of crystallinity was monitored on prepreg samples of 30–40 mg by calorimetric analysis, using a differential scanning calorimeter (DSC), Mettler DSC 30, operating from $-50\,^\circ C$ to $+450\,^\circ C$ in a nitrogen atmosphere. The material shows a T_g of $85\,^\circ C$ and a value of $T_m^0 = 303\,^\circ C$ is assumed from literature data [26].

Preliminary DSC analysis of the as-received material confirmed that it can be considered fully amorphous. In isothermal melt crystallization experiments the sample was molten for 10 min at $320\,^\circ C$ and then rapidly cooled to the test temperature. The same melting history was used for non-isothermal crystallization experiments. Cold crystallization tests were performed by heating the originally amorphous material above T_g.

Suitable experimental data were obtained between 120 and $135\,^\circ C$ (cold crystallization) and between 230 and $245\,^\circ C$ (melt crystallization). Accurate data in non-isothermal experiments were obtained at cooling rates not higher than $30\,^\circ C\,min^{-1}$.

4. Results and discussion

4.1. Nucleation behaviour

An isothermal DSC thermogram obtained on the PPS carbon fibre reinforced prepreg is shown in Fig. 1. The delay in the DSC signal represents an induction time, a relevant parameter from a processing point of view, associated with crystal nucleation. Furthermore, the induction time may be considered as the only detectable macroscopic parameter representative of the nucleation process. Following the general approach discussed for nucleation and crystallization growth, the following dependence of the induction time (t_i) on

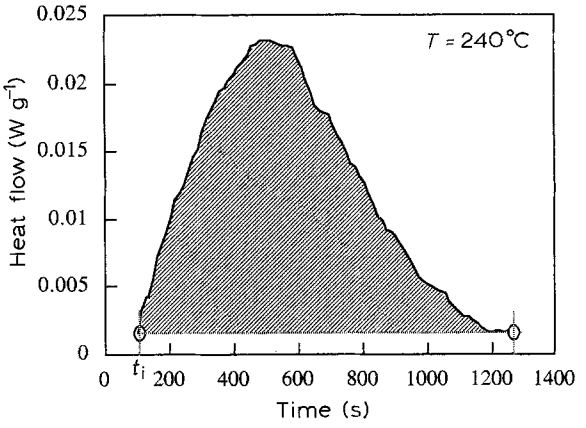

Figure 1 Isothermal DSC thermogram at 240 °C.

TABLE I Parameters of the full kinetic model (Equations 5 and 11–13)

$\ln(K_{t0}) = -3.2$ s	$E_{t1} = 410$ K^{-1}	$E_{t2}/R = 205$ K^{-1}
$T_g = 358$ K	$T_m^0 = 576$ K	$n = 1.9$
$\ln(K_0) = 4.1$ s^{-n}	$E_1 = 900$ K^{-1}	$E_2/R = 320$ K^{-1}

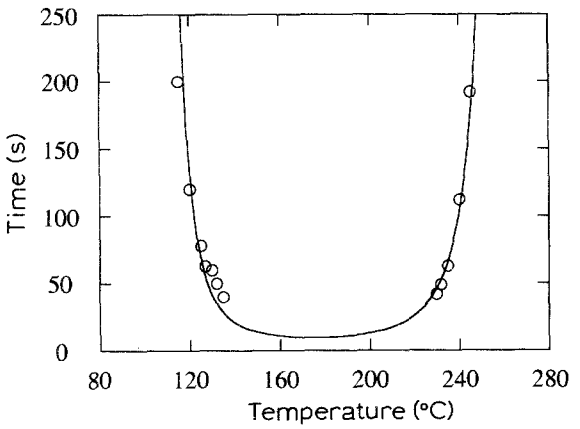

Figure 2 Induction times as a function of temperature; comparison between experimental data and model results.

temperature is proposed

$$t_i = K_{t0}\exp[E_{t2}/R(T - T_g)]\exp[E_{t1}/(T_m^0 - T)] \quad (11)$$

Induction times obtained in isothermal DSC experiments performed at different temperatures have been used to compute the parameters of Equation 11 by linear regression (Table I). A good agreement between experimental data and model results is observed in Fig. 2. From these results it is evident that the temperature range that can be explored is limited by the strong dependence of induction times on the test temperature and that also information provided by non-isothermal experiments should be considered for full model verification.

In non-isothermal conditions the induction time is given by the time, t, that satisfies the following condition

$$\int_0^t dt/t_i = 1 \quad (12)$$

where t_i is the isothermal induction time given by Equation 11 and the time $t = 0$ is taken at the melting temperature. Equations 11 and 12 will be combined with the crystal growth model in the following section.

4.2. Crystal growth behaviour

A differential expression for the rate of crystallization must be able to fit isothermal and non-isothermal data and at the same time must contain the lowest number of adjustable parameters. In this study the crystallization model given by Equation 5 is adopted with an original expression for the kinetic constant, $k(T)$. As previously mentioned, the main problems arising for simulation of the crystallization process are essentially related to the expression assumed for the kinetic constant and to the choice of the correct initial conditions for the integration of the differential model.

TABLE II Parameters obtained for Equation 8 by Hoffman *et al.* [8] and for Equation 14 (correlation coefficient on linearized Equation 14 $R = 0.996$).

Equation 8		
$T_\infty = 333.5$ K	$T_m^0 = 515.2$ K	
$\ln(G_0) = -3.62$ cm s^{-1}	$K_g = 1.2\times10^5$ K^2	$U/R = 785$ K^{-1}
Equation 14		
$T_g = 363.5$	$T_m^0 = 515.2$ K	
$\ln(G_{g0}) = -8.27$ cm s^{-1}	$E_{g1} = 221$ K	$E_{g2}/R = 221.3$ K

The problem of the initial conditions is solved by introducing the induction time (Equations 11 and 12), while a modification of Equation 9 is proposed for the kinetic constant. In fact, Equation 9 is able to represent experimental kinetic constants essentially because it shows a bell-shape between T_∞ and T_m [11, 27], being zero at the glass transition temperature and at the melting point. The same behaviour is expected if, following the previous discussion, T_∞ is replaced by T_g. Finally, the last term of Equation 9 can be simplified by keeping only the driving force for melt crystallization, represented by $T_m^0 - T$. Then, the following macrokinetic expression is proposed for the temperature dependence of k

$$k = k_0 \exp[-E_2/R(T - T_g)] \times \exp[-E_1/(T_m^0 - T)] \quad (13)$$

This equation contains only three parameters and their calculation is simplified compared with Equation 9. The same approach as was used for the development of Equation 13 can be adopted to modify Equation 8 for the linear crystal growth rate

$$G = G_{g0} \exp[-E_{g2}/R(T - T_g)] \times \exp[-E_{g1}/(T_m^0 - T)] \quad (14)$$

Equation 14 can be compared with Equation 8 by using the results obtained by Hoffman *et al.* [8] for polystyrene. The parameters of both equations are reported in Table II while their predictions are well compared in Fig. 3, indicating the ability of the simplified Equation 14 model to represent the crystallization behaviour with the same accuracy as Equation 8, and then confirming the validity of the approach used to model the temperature dependence of the kinetic constant in Equation 13.

Further verification of Equation 13 predictions, using parameter values computed by linear regression, reported in Table I, is presented in Figs 4 and 5, where a reasonable agreement between experimental and theoretical results is observed. In particular, kinetic constants measured in isothermal experiments and Equation 13 results are compared in Fig. 4, where it is shown that only a limited amount of experimental data can be obtained in two narrow temperature ranges (cold and melt crystallization). On the other hand, kinetic constant values calculated from DSC experiments performed at constant cooling rates (5 °C min^{-1} and 30 °C min^{-1}) are shown in Fig. 5 compared with model results.

The ability of the full model (Equations 5, 11, 12 and 13) to represent experimental data under isothermal

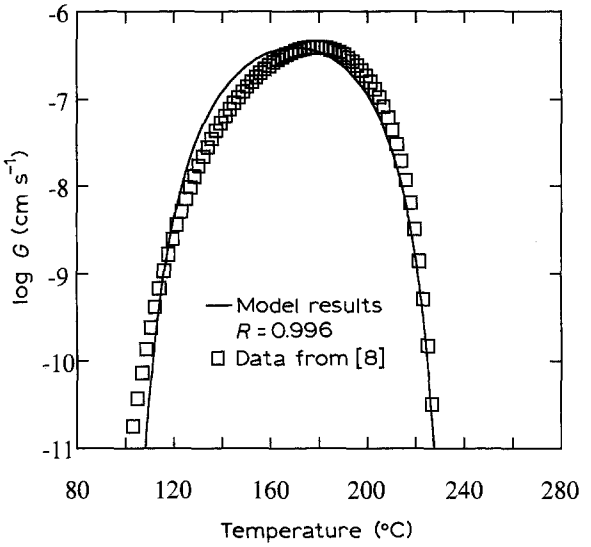

Figure 3 Comparison between linear growth rate values calculated for polystyrene using the model developed by Hoffman *et al.* [8] (Equation 8) and the results of Equation 14.

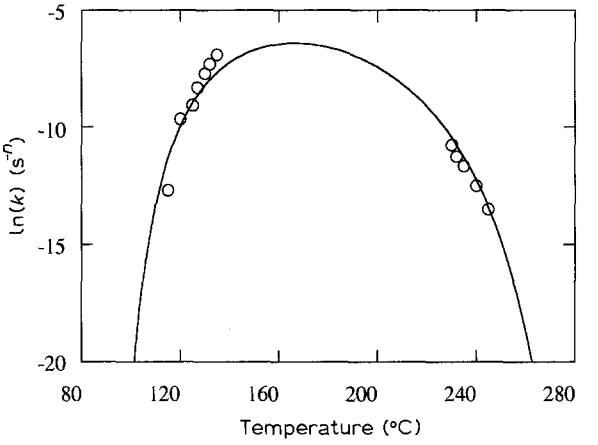

Figure 4 Comparison between kinetic constants evaluated in isothermal DSC experiments and model predictions (Equation 13).

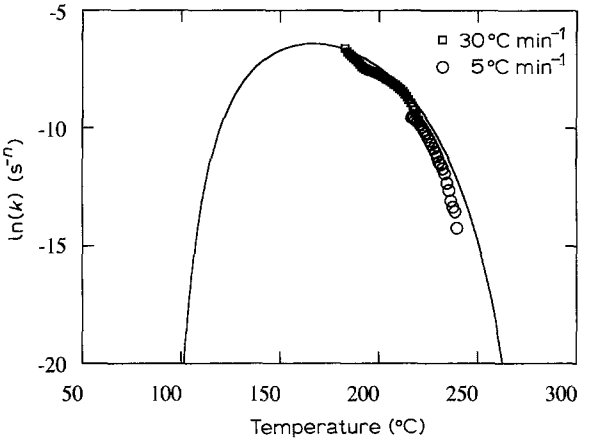

Figure 5 Comparison between kinetic constants evaluated in non-isothermal DSC experiments (5 and 30 °C min^{-1}) and model predictions (Equation 13).

and non-isothermal conditions is shown in Figs 6–10. It can be noted that the onset of crystallization is well predicted by the induction time model in isothermal as well as in non-isothermal experiments, indicating that the nucleation process is correctly represented by this

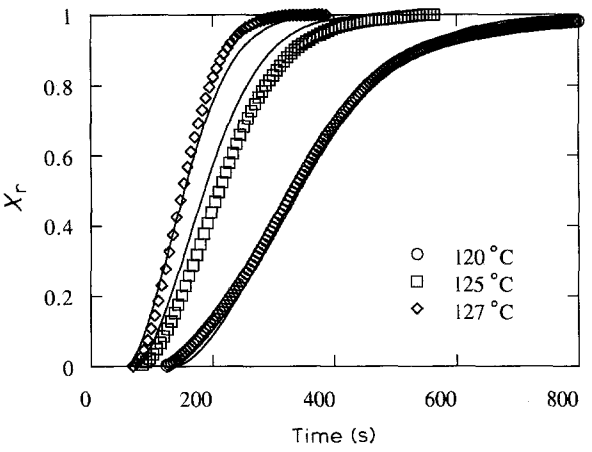

Figure 6 Comparison between experimental data and theoretical prediction of the full model for isothermal cold crystallization.

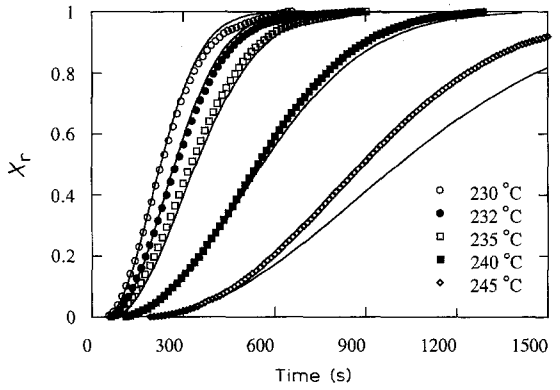

Figure 7 Comparison between experimental data and theoretical prediction of the full model for isothermal melt crystallization.

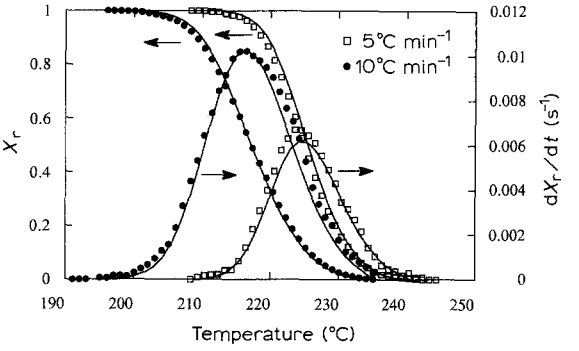

Figure 8 Comparison between experimental data and theoretical prediction of the full model for non-isothermal crystallization at constant cooling rate (5 and 10 °C min^{-1}).

macrokinetic approach. The full model shows a very good agreement with experimental data obtained under very different thermal conditions, providing a fundamental tool for the study of the processing of semi-crystalline thermoplastic matrix composites.

5. Time temperature transformations

Solid state phase transformations governed by slow kinetic processes are usually studied in metallurgy using plots called TTT (time–temperature transformations) for isothermal processes or CCT (continuous cooling transformations) when a constant cooling rate

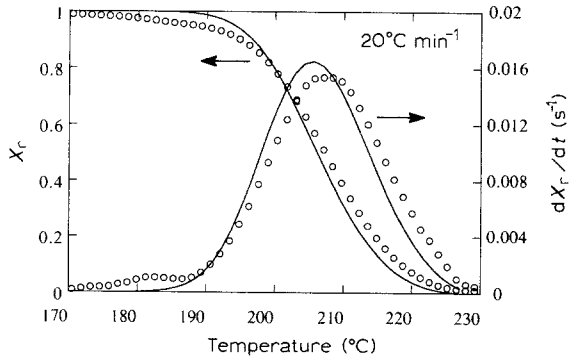

Figure 9 Comparison between experimental data and theoretical prediction of the full model for non-isothermal crystallization at constant cooling rate (20 °C min^{-1}).

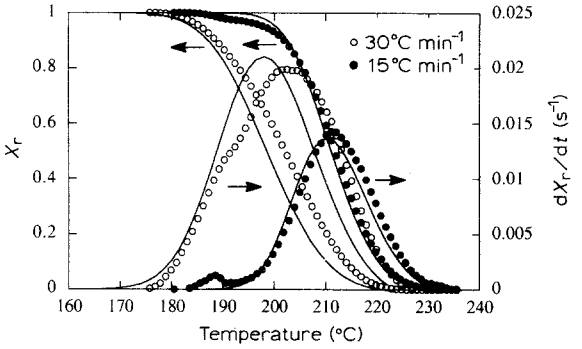

Figure 10 Comparison between experimental data and theoretical prediction of the full model for non-isothermal crystallization at constant cooling rate (15 and 30 °C min^{-1}).

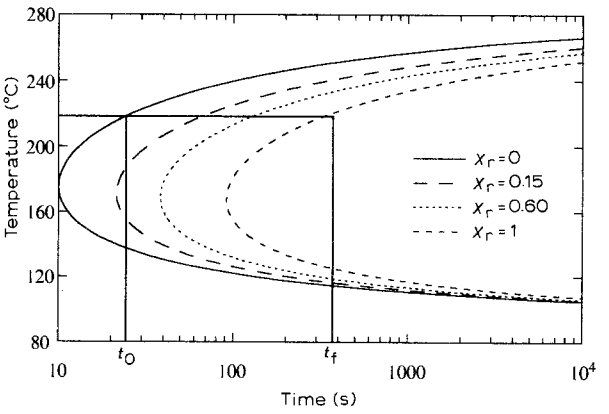

Figure 11 Isothermal TTT (time–temperature transformation) diagram for crystallization of the PPS matrix composite studied.

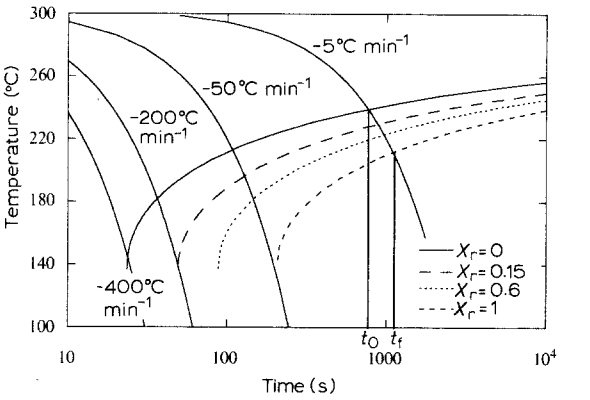

Figure 12 Non-isothermal CCT (constant cooling transformation) diagram for crystallization of the PPS matrix composite studied.

is applied [28]. The same kind of approach has been used by Gillham [29] for the chemorheology of thermosetting matrices, in order to predict gelation and vitrification phenomena during cure of composite matrices. Also, the crystallization kinetics of polymers may be better understood using this kind of approach, as reported by White *et al.* [30, 31]. They found different curves for the onset of crystallization between quiescent melt crystallization and crystallization under high strain rates occurring in injection moulding or melt spinning of polymers. However the TTT and CCT diagrams reported in those papers are only a qualitative representation of the experimentally observed behaviour and give information only about the onset time of crystallization.

The model developed in this paper can be used to build TTT and CCT plots. A TTT diagram for the crystallization of the PPS matrix composite studied is reported in Fig. 11. The first curve from the left represents the beginning of crystallization and it is obtained as the locus of points given by Equation 11. The curves corresponding to a given degree of crystallization ($X_r = 0.15$, $X_r = 0.30$, etc.) are computed by application of Equations 5, 11 and 13. At a fixed temperature, a horizontal line gives, at the first intersection, the time (t_0) to reach the onset of the crystallization process ($X_r = 0$) in accordance with the induction time model. Then the kinetic model for crystal growth provides the time needed to reach different degrees of crystallization and finally the time (t_f) for full crystallization ($X_r = 1$). It should be noted that the time required to reach $X_r = 1$ is infinite, and so the curve corresponding to full crystallization has been calculated for $X_r = 0.999$.

It must be underlined that TTT plots are obtained under isothermal conditions and, therefore, they can be rigorously used only for isothermal processes. For more complex thermal conditions, Equations 5, 11, 12 and 13 must be integrated in order to obtain a time–temperature plot. In particular, the crystallization behaviour during constant cooling rate processes (CCT plot) is described in Fig. 12, where curves representing different degrees of crystallization are plotted as a function of time. Each point on these curves has been obtained by integration of the full model at a given cooling rate. Then, the intercept of a constant degree of crystallization curve with a constant cooling rate curve represents the time needed for the material to reach the given degree of crystallization under the specified thermal conditions. Moreover, the model is able to predict full quenching of the PPS composite matrix when the continuous cooling curve misses the curve representative of the onset of crystallization ($X_r = 0$). In particular, Fig. 12 indicates that a fully amorphous material is obtained for cooling rates higher than 400 °C min^{-1}, a quasi amorphous material ($X_r < 0.05$) is developed at a cooling rate higher than 200 °C min^{-1} and the limiting cooling rate for full crystallization is lower than 50 °C min^{-1}. Both TTT and CCT plots must be used when a complex

thermal history is imposed as a combination of isothermal and constant cooling rate processes. More complex thermal processing conditions cannot be represented in simple diagrams and an individual integration of the full model must be performed to obtain quantitative results.

A different representation of CCT plots (Fig. 13) can be obtained indicating on the ordinate the temperature derivative dT/dt (constant cooling rate). The crystallization behaviour at a given cooling rate can be obtained in this diagram simply by drawing a horizontal line.

In this framework TTT and CCT plots provided by the material suppliers, for each semicrystalline polymer or composite matrix, could represent a fundamental tool in order to determine the best process conditions. Nowadays, material standardization represents a major need for the users of composite material in order to assess their properties and to determine the correct process conditions required by each technology.

Finally, it must be recognized that the kinetic analysis presented in this work takes regard only of kinetic behaviour as detected by calorimetric techniques. This study should be combined with morphological information obtained at different crystallization temperatures and under different cooling rates in order to complete the TTT and CCT plots. In fact, it is well known that, depending on the degree of undercooling, crystals with different spherulite size and lamellar thickness can be developed [7]. Moreover, isothermal dynamic mechanical crystallization experiments suggest that the mechanical properties increase at long times, even if the crystallinity measured by DSC is apparently fully developed [32].

6. Conclusions

A macrokinetic model for the crystallization of a polyphenylene sulphide (PPS) matrix for high performance composites has been developed. The model, accounting for the induction time due to nucleation, is able to predict the crystallization behaviour under isothermal and non-isothermal conditions, including cold and melt crystallization, and quenching effects. Moreover, the simple expression proposed for the temperature dependence of the kinetic constant allows a straightforward calculation of model parameters. Theoretical results are in good agreement with calorimetric experimental data obtained under a wide range of thermal conditions.

Finally, time–temperature transformation plots, constructed from the model developed for isothermal (TTT) and non-isothermal (CCT) conditions, provide a fundamental tool for understanding the crystallization behaviour of semicrystalline matrices and to determine the most adequate processing conditions.

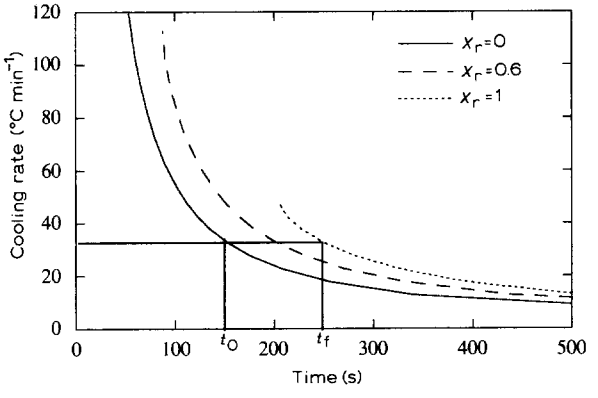

Figure 13 Different form of the CCT (constant cooling transformation) diagram reported in Fig. 12 obtained indicating on the ordinate the temperature derivative dT/dt.

7. Acknowledgements

The financial support of Alenia Saipa is gratefully acknowledged.

References

1. N. J. JOHNSTON and P. M. HERGENROTHER, in Proceedings of the 32nd International SAMPE Symposium, April 1987 p. 1400.
2. C. VELISARIS and J. C. SEFERIS, *Polym. Engng Sci.* **26** (1986) 1574.
3. J. M. KENNY, A. D'AMORE, L. NICOLAIS, M. IANNONE and B. SCATTEIA, *Sampe J.* **25** (1989) 27.
4. A. MAFFEZZOLI, J. M. KENNY and L. NICOLAIS, *ibid.* **25** (1989) 35.
5. J. M. KENNY and A. MAFFEZZOLI, *Polym. Engng Sci.* **31** (1991) 607.
6. *Idem. Compos. Polym.* **4** (1991) 12.
7. B. WUNDERLICH, "Macromolecular Physics" (Academic Press, New York, 1976).
8. J. D. HOFFMAN, G. T. DAVIS and J. I. LAURITZEN, in "Treatise on Solid State Chemistry", edited by N. B. Hannay (Plenum Press, New York, 1976) Vol. 3, Ch. 7.
9. Y. LEE and R. S. PORTER, *Macromolecules* **21** (1988) 2770.
10. D. R. BUDGELL and M. DAY, *Polym. Engng Sci.* **31** (1991) 1271.
11. L. C. LOPEZ and G. L. WILKES, *J. Rev. Macromol. Chem. Phys.* **C29**(1) (1989) 83.
12. A. MAFFEZZOLI, J. M. KENNY and L. NICOLAIS, *Therm. Acta* **199** (1992) 133.
13. Y. LEE and R. S. PORTER, *Polym. Engng Sci.* **26** (1986) 633.
14. G. P. DESIO and L. REBENFELD, *J. Appl. Polym. Sci.* **39** (1990) 825.
15. K. NAKAMURA, K. KATAYAMA and T. AMANO, *ibid.* **17** (1973) 1031.
16. R. M. PATEL and J. E. SPRUIELL, *Polym. Engng Sci.* **31** (1991) 730.
17. M. R. KAMAL and E. CHU, *ibid.* **23** (1983) 27.
18. C. C. LIN, *ibid.* **23** (1983) 113.
19. T. OZAWA, *Polymer* **12** (1971) 150.
20. A. Y. MALKIN, V. P. BEGHISHEV, I. A. KEAPIN and S. A. BOLGOV, *Polym. Engng Sci.* **24** (1984) 1396.
21. A. Y. MALKIN, V. P. BEGHISHEV, I. A. KEAPIN and Z. S. ANDRIANOVA, *ibid.* **24** (1984) 1402.
22. I. H. HILLIER, *J. Polym. Sci.* **A3** (1965) 3069.
23. P. CEBE, *Polym. Engng Sci.* **28** (1988) 1192.
24. *Idem, Polym. Compos.* **28** (1988) 271.
25. S. S. SONG, J. L. WHITE and M. CAKMAK, *Polym. Engng. Sci.* **30** (1990) 944.
26. A. J. LOVINGER, D. D. DAVIS and F. J. PADDEN, *Polymer* **26** (1985) 1595.
27. L. C. LOPEZ and G. L. WILKES, *ibid.* **29** (1988) 106.
28. L. H. VAN VLACK, "Elements of Material Science", 2nd Edn (Addison-Wesley, Reading, MA, 1964).

29. J. B. ENNS and J. K. GILLHAM, *J. Appl. Polym. Sci.* **28** (1983) 2567.
30. J. E. SPRUIELL and J. L. WHITE, *Polym. Engng Sci.* **15** (1975) 660.
31. C. M. HSIUNG, M. CAKMAK and J. L. WHITE, *Int. Polym. Proc.* **5** (1989) 109.
32. J. M. KENNY, A. MAFFEZZOLI and L. NICOLAIS, *Polym. Compos.* **13** (1992) 386.

Received 21 July 1992
and accepted 4 January 1993